Materials Science and Engineering A 527 (2010) 1970–1974

Contents lists available at ScienceDirect

Materials Science and Engineering A

journal homepage: www.elsevier.com/locate/msea

Effects of hot rolling processing on microstructures and mechanical properties of Mg–3%Al–1%Zn alloy sheet

L. Jin[a,b,*], J. Dong[a,b], R. Wang[a,b], L.M. Peng[a,b]

[a] National Engineering Research Center of Light Alloy Net Forming, Shanghai Jiao Tong University, P.R. China
[b] Key State Laboratory of Metal Matrix Composite, Shanghai Jiao Tong University, P.R. China

ARTICLE INFO

Article history:
Received 12 April 2009
Received in revised form
11 November 2009
Accepted 20 November 2009

Keywords:
AZ31 Mg alloy
Hot rolling
Grain refinement
Twinning
Texture

ABSTRACT

The microstructure evolution and deformation mechanisms of AZ31 alloy sheet during hot rolling were investigated. The initial microstructure in the as-received AZ31 sheet shows basal texture with an average grain size of 37 μm. During the subsequent hot rolling processing, dislocation slip occurs in addition to extension, contraction and double twinning, and the twinning mode is dependent on the grain orientation, grain size and rolling temperature. Continuous dynamic recovery and recrystallization (CDRR) is the main mechanism of grain refinement for the AZ31 sheet during hot rolling, and the $\{-1\,0\,1\,1\}$ contraction and $\{-1\,0\,1\,1\}-(1\,0\,-1\,2)$ double twinning accelerate the refinement process. Contraction and double twinning have positive effect on grain refinement and texture randomization for the AZ31 alloy during hot rolling. In this study, higher per-pass reduction of 50% and higher rolling temperature of 400 °C led to more uniform grain structure with more random texture, which resulted in the higher ductility than that of the sheet samples rolled at 300 °C and at per-pass reduction of 30%. Therefore, higher temperatures and larger per-pass reduction rolling are recommended for microstructure optimization and the mechanical properties improvement of the AZ31 sheet.

1. Introduction

Magnesium sheet is currently being tested for various applications. However, rolled Mg alloys often exhibit relatively low strength and poor formability especially at room temperature due to the basal or near basal texture usually developed during rolling [1]. Fine grains and randomized texture are two important requirements for the application of Mg alloy sheet. Texture evolution in Mg alloys is affected by the interaction between the strain path and the initial microstructure [2], and the activation of basal slip has been considered as the reason for the basal texture in Mg alloy sheet [3]. It was also reported that the basal texture originated from the $(1\,0\,-1\,2)$ extension twinning based on the assumption that twinning would reorient the *c*-axes parallel to the compressive stress, supported by experiments [4] and simulations [5]. While it is very difficult to change the basal texture of magnesium sheet, such as AZ31 and AZ61 alloys, the intensity of the basal texture can be weakened and the grain size could be reduced by controlling the rolling processing if the correlation between the deformation modes and rolling processing parameters could be established.

Mg is known to deform by slip, twinning and grain boundary sliding (GBS). GBS is probably available for the superplastic deformation or in the nano-materials [6], and it has been observed in fine-grained AZ31 as well [7–9]. The dislocation slip on basal planes can lead to large plastic deformation, but there are only two independent basal slip systems [10,11], far fewer than the five independent systems necessary for general deformation [12]. Twinning has been considered providing additional deformation in magnesium and $\{1\,0\,-1\,2\}\langle 1\,0\,-1\,1\rangle$ extension twinning and $\{1\,0\,-1\,1\}\langle 1\,0\,-1\,2\rangle$ contraction twinning are frequently reported in Mg and Mg alloys [13]. In the case of dislocation slip, prismatic $\{1\,0\,-1\,0\}\langle 1\,1\,-2\,0\rangle$, and pyramidal $\{1\,0\,-1\,1\}\langle 1\,1\,-2\,0\rangle$ systems can be operated in the AZ31 alloys in addition to slip in basal $(0\,0\,0\,1)\langle 1\,1\,-2\,0\rangle$ system. For the AZ31 sheet rolled at elevate temperatures, non-basal dislocation slip and other twinning modes are easily activated in addition to basal slip and extension twinning, and the deformation mode in the AZ31 alloy sheet during hot rolling are strongly dependent on the initial grain structure and the rolling processing. In addition, continuous dynamic recovery and recrystallization (CDRR) has been reported as a phenomenon for the grain refine and growth in Mg alloys during deformation at elevate temperatures [14–15], according to the low energy dislocation theory (LED's) [16]. However, the correlation between the rolling processing, deformation mechanisms, and the microstructure evolution, is not well understood. Fortunately the electron backscattered diffraction (EBSD) technique provides the possibility to follow the

* Corresponding author at: School of Material Sciences and Engineering, Shanghai Jiao Tong University, 800 Dongchuan Road, Shanghai, 200240, China.
E-mail address: j_jinli@sjtu.edu.cn (L. Jin).

0921-5093/$ – see front matter © 2009 Elsevier B.V. All rights reserved.
doi:10.1016/j.msea.2009.11.047

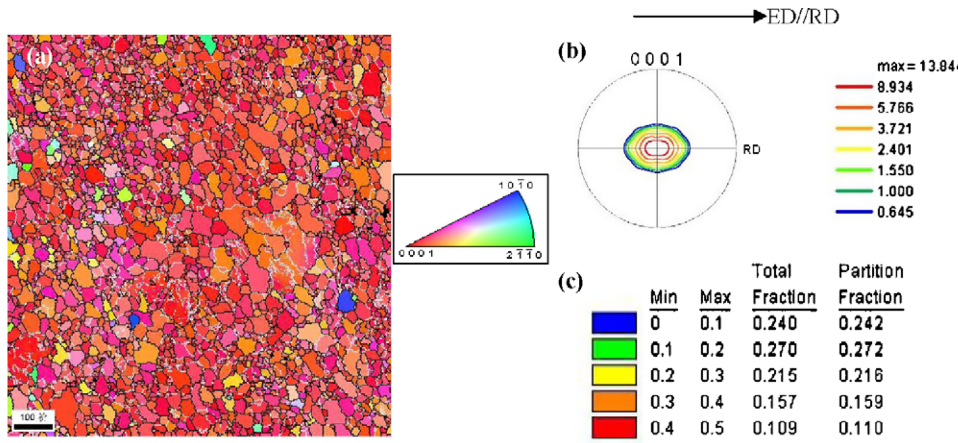

Fig. 1. Initial microstructures of AZ31 alloy sheet: (a) IPF map, (b) pole figures and (c) Schmid factor fractions subject to basal slip system.

evolution of twins, misorientation, texture and grain structure of the AZ31 sheet during hot rolling, and the evidence for understanding the effect of deformation mechanisms on the microstructures evolution. This will open up the possibility of controlling the mechanical response by designing microstructure appropriate to rolling processing. Therefore, this paper aimed at the microstructure evolution of AZ31 alloy during hot rolling using EBSD, and the correlation between the microstructure and mechanical properties.

2. Materials and experiments

The alloy used in this study was AZ31 alloy. Prior to hot rolling, the alloy was hot-extruded at 573 K to a rectangular bar with a cross-section of 110 mm × 10 mm. Fig. 1 shows the initial microstructure of the AZ31 alloy before hot rolling, including the inverse pole figure (IPF) map, pole figures and Schmid Factor Fractions. The results indicate a primarily basal texture with the *c*-axes nearly perpendicular to the sheet plane and only a few grains with their *c*-axes parallel to the sheet plane and the original extrusion direction (ED). Fig. 1 (c) shows the Schmid Factor value of majority grains is less than 0.3, suggesting that the grain orientation is not favorable for basal slip.

The extruded bar was pre-heated at 573 or 673 K for 0.5 h, respectively, and then hot-rolled to the thickness of 3.5 and 2.5 mm in hot rolling mills at a given reduction of 30% or 50% per pass, respectively. The temperature of the rollers was controlled at about 473 K using internal electric heaters. The total thickness reduction was about 65% and 75%, respectively. The rolled plates were reheated between passes to maintain the workability. The rolling direction was parallel to the extrusion direction of the as-received bars. The rolling specimens were water-quenched immediately after each pass. And small samples were taken from the quenched specimens for EBSD analysis using a LEO^{TM} 1450 Scanning electron microscope operated at 20 kV fitted with a TSL^{TM} EBSD camera [17]. Due to the deformation structure in the EBSD sample, there is low index quality on the areas with more dislocation reactions and finer twins, but the results still can give a lot of useful information.

3. Results and discussion

Fig. 2 shows the grain size distribution at various per-pass reductions and rolling temperatures. The initial extrusion material has coarse grains ranging from 10 to 160 μm and an average grain size of 37.29 μm. Fig. 2(a) shows the grain structure evolution after rolling 1, 2 and 3 passes at a temperature of 300 °C and at a per-pass reduction of 30%. After the single-pass rolling, the average grain size was greatly reduced with the majority of grains in the 10–30 μm range but a considerable amount of large grains ranging from 40 to 85 μm. After 2 passes of rolling, the grains were more uniformly refined with an average grain size of 8.8 μm. A further rolling pass actually caused a slight increase of grain size to 13 μm. Similar results were obtained at the 400 °C rolling. Fig. 2(b) summarizes the average grain sizes of AZ31 sheet after hot rolling at various per-pass reductions and rolling temperatures. The results show that at a given rolling pass, the average grain sizes for the sheet rolled at 400 °C are larger than that of 300 °C-rolled sheet, and that higher per-pass reduction led to finer grains at the similar total thickness reduction and at same rolling temperature.

Fig. 3 shows the actual tension plots of AZ31 alloy sheet before and after hot rolling. The stress–strain curves exhibit that there are weaker strain hardening behaviors and higher yield stress (YS) and ultimate tensile strength (UTS) in rolled AZ31 alloy sheet than

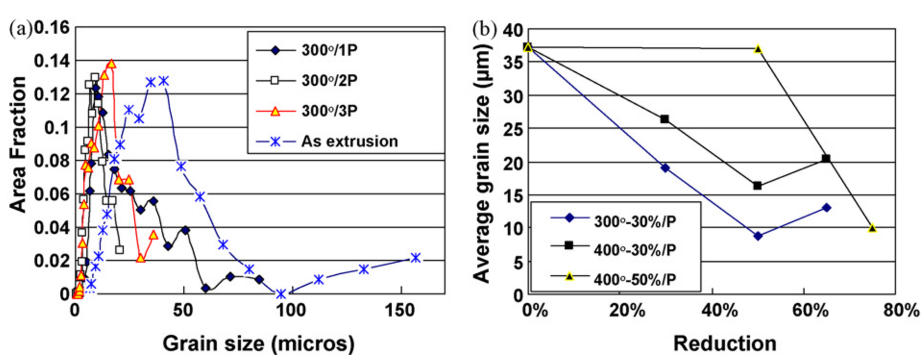

Fig. 2. (a) The distribution of grain sizes of AZ31 alloy sheet after hot rolling 1–3 pass at 300 °C with per-pass reduction of 30%, and (b) average grain sizes at various rolling processing, in which grains were divided by grain boundaries with misorientation larger than 15°.

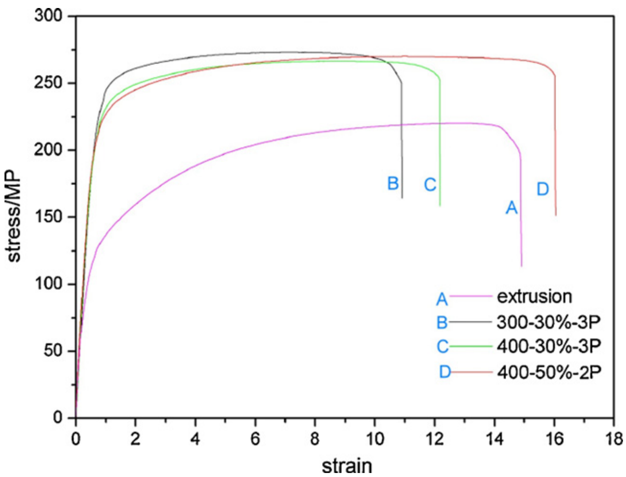

Fig. 3. Stress–strain curve of AZ31 sheet before and after hot rolling.

that in as-extrusion sheet. The rolling AZ31 sheets have similar YS and UTS, but have significant difference in their ductility, which is substantially higher in the sample after hot rolling at higher temperature and larger per-pass reduction.

Fig. 4 shows the IPF maps of AZ31 alloy sheet after hot rolling 1 pass at 300 °C and 30% reduction and at 400 °C with 30% and 50% reductions, respectively. Grain boundaries were defined as high angle grain boundaries (HAGB) with misorientation of 15–90° and lower angle grain boundaries (LAGB) with misorientation of 2–15°, and HAGB was shown as black lines and LAGB was shown as write lines in the IPF map in Fig. 4. The calculated grain sizes in Fig. 2 are for those grains divided by HAGB. Fig. 4(a) shows that the microstructure was progressively refined although some coarse grains remained after the 30% rolling reduction at 300 °C. The fine grains form typical necklace structures due to the strain accumulation during rolling which lead to CDRR in these regions. More coarse grains were observed in Fig. 4(b) and (c) after rolling 1 pass at 400 °C with per-pass reduction of 30% and 50%. As shown in Fig. 4(c), a large number of LAGBs in the coarse grain interiors, are likely the result of the dislocation slip and interactions, which could develop into HAGB and grain refinement during further deformation according to the continuous dynamic recovery and recrystallization (CDRR) model [14,15]. This is consistent with the data in Fig. 2(b) that the larger average grain sizes were obtained in the sheet after 1 pass rolling at 400 °C and at per-pass reduction of 50% but the finest average grains were observed after rolling 2 passes at this condition.

Fig. 4 also shows some twinning sites during the hot rolling, but it is difficult to identify the twinning modes due to the lower resolution. The microstructure as shown in the black box in Fig. 4(c) was analyzed by EBSD at a smaller step size of 0.5 μm, and the result is shown in Fig. 5. Fig. 5(a) and (b) shows the IPF maps with the lattice orientation and grain shape maps with defined twin boundaries. It can be seen from the figures that twinning nucleated in grain 1, 2 and 3, and the twining mode is $\{1\,0\,{-1}\,2\}\langle{-1}\,0\,1\,1\rangle$ extension twinning in grain 1, and $\{-1\,0\,1\,1\}-\{1\,0\,{-1}\,2\}$ double twinning in grains 2 and 3 according to the twin boundary definition. The parent grains 2 and 3 were divided by the double twins, and then the initial grains were refined to 3 or 5 finer grains as a result. The results suggest that the twinning in this process, especially the contraction and double twinning, accelerates the processing of grain refinement. The twin-induced phenomenon could be explained as following. More twin boundaries develop after twinning, which could be the obstacles for dislocation slip during straining. Towards the twin boundaries density of dislocations and misorientations increase, and at high strains, HAGBs may develop, and then resulted in the grain refinement. As Humphreys said [15], dynamic recrystallization originates at high angle boundaries regardless of the details of the mechanism of nucleation. But the grain nucleation and growth here may still follow the mechanism of CDRR with the sub-grain formation and then fine-grain with HAGB.

Fig. 6 shows the grain shape maps with defined twin boundaries of the AZ31 alloy sheet after rolling 3 passes with per-pass reduction of 30% at 300 °C and 400 °C, and rolling 2 passes with per pass reduction of 50% at 400 °C, respectively. The grain size is larger in Fig. 6(b) compared to Fig. 6(a) and (c), indicating that the grains were refined further by higher per-pass reduction rolling and at a lower temperature. The fact that smaller grain size is found at higher reduction is due to stored energy of deformation being higher which leads to higher driving force for nucleation and hence finer grain size. At the lower temperature the softening rate is slower, hence leads to higher work hardening and larger driving force for nucleation of grains, and here grain growth is also slow.

In addition, contraction twins, double twins and extension twins were observed in the larger grains in Fig. 6, and there is a higher volume fraction of contraction twins and double twins than that of extension twins, especially there are less extension twins at the higher rolling temperature. Fig. 6 also shows that the twinning mode is dependent on the grain size. Twinning is more visible in the parent grains with gain size larger than 20 μm, however, few or no twins were observed in smaller grains as shown in Fig. 6(c).

As shown in Fig. 1, the initial grain orientations of the AZ31 alloy sheet are not favorable for the dislocation slip on the basal plane; in addition, the majority of the grains have their *c*-axis parallel to the compressive stress, which is not favorable for the extension twinning in those grains. But the basal slip is still the main deformation mode due to the lowest critical resolved shear stress (CRSS), and also the contraction twinning can be possibly activated ascribe to the *c*-axes of those grains under compression. In the case of a few grains, blue or green grains in Fig. 1(a) with their *c*-axes paral-

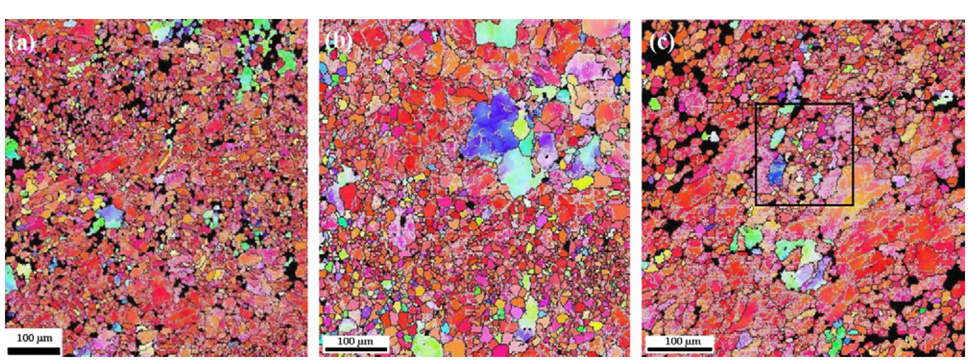

Fig. 4. IPF maps of AZ31 alloy sheet after rolling at (a) 300 °C with reduction of 30%, (b) 400 °C with reduction of 30% and (c) 400 °C with reduction of 50%.

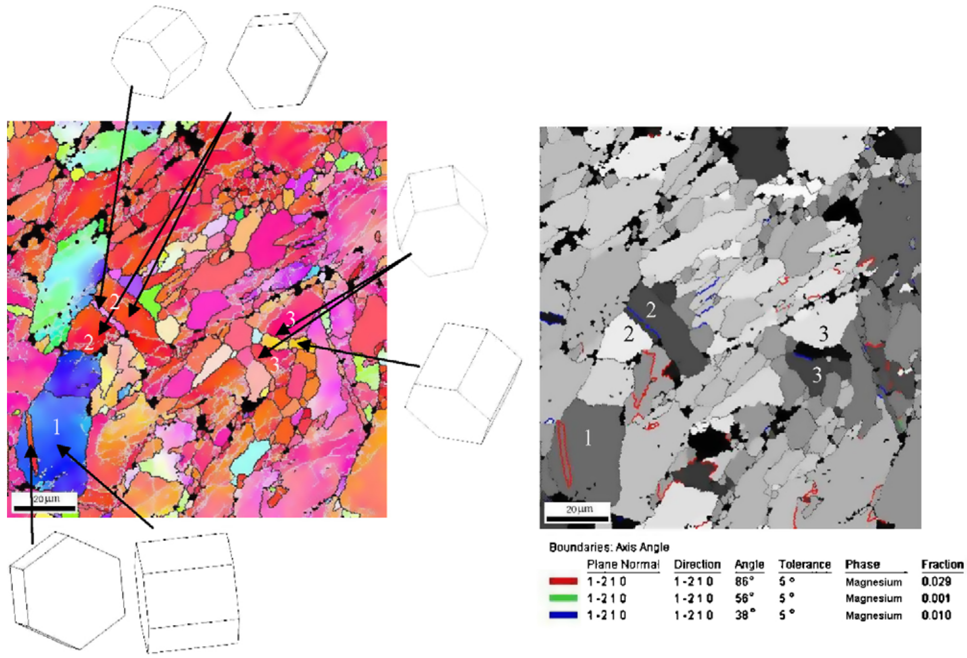

Fig. 5. Microstructures of AZ31 alloy sheet rolled 1 pass at 400 °C with reduction of 50%, (a) IPF map and the lattice orientation of the parent and twins, (b) Grain shape map with defined twin boundaries, extension twin boundaries (86° ⟨1 −210⟩ ±5°) are outlined in red, contraction twin boundaries (56° ⟨1 −210⟩ ±5°) outlined in green and the double twin boundaries (38° ⟨1 −210⟩ ±5°) outlined in blue. (For interpretation of the references to color in this figure legend, the reader is referred to the web version of the article.)

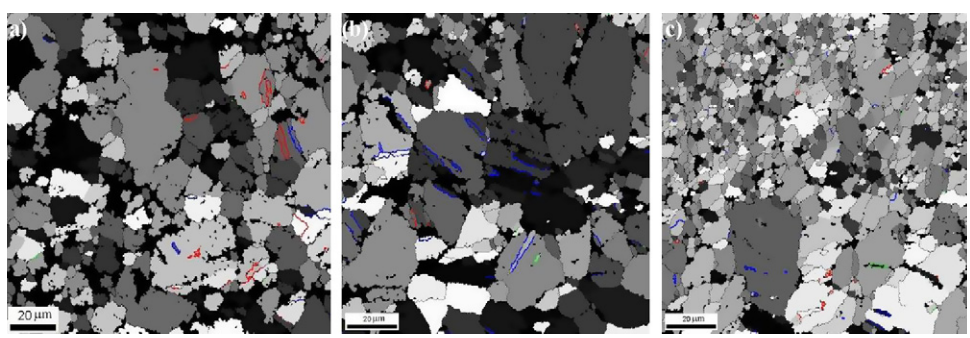

Fig. 6. Grain shape maps with twin boundaries of AZ31 alloy sheet after rolling: (a) 3 passes at 300 °C, (b) 3 passes at 400 °C with per-pass reduction 30%, and (c) 2 passes at 400 °C with per-pass reduction of 50%. In which the twin boundaries were defined as same as that in Fig. 5.

lel to sheet plane, {1 0 −1 2} extension twinning is easily occurred. Generally the extension twinning will be reoriented to 86 ° from the initial status [13], and, the parent grain will be replaced by the extension twins due to the fast twin growth. In the new twins after extension twinning, only dislocation slip on basal plane and contraction twinning are possible due to the new grain orientation. In the case of {−1 0 1 1} contraction twinning, the twins have a misorientation of 56° with the parent grains, and the contraction is thinner and longer than extension twins and, thus, is difficult for twin growth. However, the new grain orientations are more favorable for extension twinning and dislocation slip on basal slip system after contraction twinning. Therefore, the {1 0 −1 2} extension twinning always follows the {−1 0 1 1} contraction twinning during deformation in Mg alloy, i.e., the {−1 0 1 1} − {1 0 −1 2} double twinning. The double twins have misorientation of near 38° with the parent grain [13]. As a result, there are more double twins than contraction twins in the AZ31 sheet after hot rolling as shown in Fig. 6.

As shown in Fig. 7, the twinning modes are also dependent on the rolling temperature. Fig. 7(c) shows the volume fraction of the contraction and double twins in the AZ31 alloy sheet after hot rolling, and the highest volume fraction of double and contraction twins was found in the sheet after rolling 3 passes at 400 °C with the per-reduction of 30%, while the lowest volume fraction in the sheet after rolling 3 passes at 300 °C with same per-pass reduction. The results suggest that contraction and double twinning are readily activated at higher rolling temperatures, which could be ascribe to the lower CRSS for the contraction and double twinning at higher temperature as similar as the CRSS for non-basal dislocation slip comparing

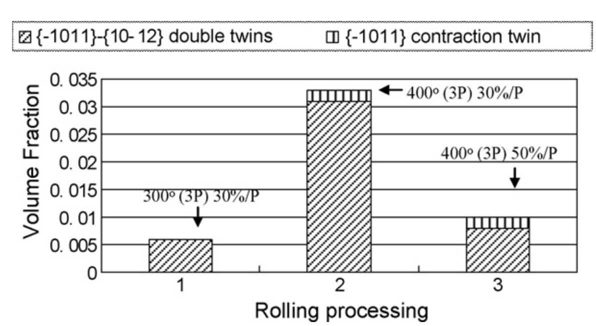

Fig. 7. The volume fraction of contraction and double twins in the AZ31 sheet after hot rolling.

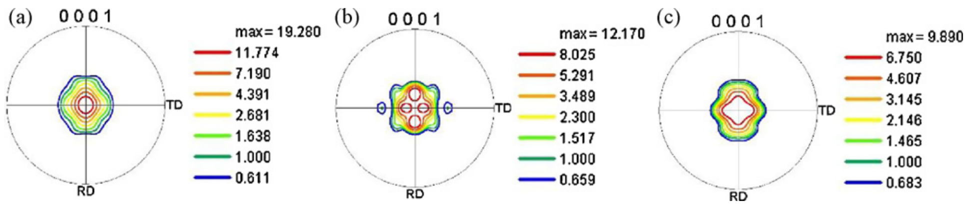

Fig. 8. (0 0 0 1) pole figures of AZ31 alloy sheet after rolling (a) 3 passes at 300 °C, (b) 3 passes at 300 °C with per-pass reduction 30% at 400 °C, and (c) 2 passes at 400 °C with per-pass reduction of 50%.

to Basal dislocation slip [18]. On the other hand, the {1 0 −1 1} contraction and {1 0 −1 1} − {1 0 −1 2} double twinning are reoriented from the basal poles to 56° and 38° reference to initial status, and therefore the activation of the contraction and double twining in the AZ31 sheet can result in the weakening of the basal texture. Fig. 8 is the (0 0 0 1) pole figures of AZ31 after hot rolling, showing broader distribution of basal pole and weaker basal texture in AZ31 sheet rolled at 400 °C compared to the samples rolled at 300 °C. However, the change in global texture is insignificant due to the limited volume fraction of twinned material.

As mentioned before, fine grains and randomized texture are two important requirements for improved mechanical properties and the applications of the Mg alloy sheet. In this study, the grain structure can be effectively refined at lower rolling temperatures, but more extension twinning and dislocation on basal slip system were observed in this condition, resulting in higher basal texture intensity. At higher rolling temperatures, more contraction and double twinning can be activated and the non-basal slip also would accommodate larger plastic deformation [18], weakening the basal texture. Thus, higher rolling temperatures are favorable for texture randomization, but lead to larger grains at given per-pass reduction higher temperature rolling resulted. Fortunately, rolling at higher per-pass reduction can offset the large grain size. Therefore, higher temperatures and larger per-pass reductions are recommended for the AZ31 sheet alloy, to achieve better mechanical properties. The observed high ductility in Fig. 3 provides a good example based on above idea.

4. Conclusions

In summary, it was found that dislocation slip on basal plane is still the main deformation mode in AZ31 sheet during hot rolling due to the initial microstructure with basal texture. The {1 0 −1 2} extension twinning occurred in grains with their *c*-axes parallel to sheet plane and the extension twinning reoriented the grains to 86° from their initial state. The {1 0 −1 1} contraction twinning and {1 0 −1 1} − {1 0 −1 2} were activated at larger thickness reduction because the *c*-axes of majority grains were under compression during rolling. Twinning is also dependent on initial grain size and the rolling temperature, twinning is readily observed in the larger parent grains and more contraction and double twinning are activated at higher rolling temperatures. CDRR is the main mechanism of grain refinement for the AZ31 sheet during hot rolling, but the twinning in this process, especially the contraction and double twinning, accelerates the grain refinement process. Basal slip and extension twinning will induce the formation of basal texture; but contraction and double twinning have positive effect on the grain refinement and texture randomization for the AZ31 alloy during hot rolling.

In this study at a given rolling reduction, the average grain size of AZ31 sheet rolled at 400 °C was larger than that of the sheet samples rolled at 300 °C, and at same rolling temperature higher per-pass reduction led to finer grain size in the sheet materials. And higher per-pass reduction of 50% and higher rolling temperature of 400 °C led to more uniform grain structure with more random texture, which resulted in the higher ductility than that of the sheet samples rolled at 300 °C and at per-pass reduction of 30%. Therefore, higher temperatures and larger per-pass reduction rolling should be used to optimize the microstructure and improve the mechanical properties of AZ31 sheet.

Acknowledgments

The Science and Technology Commission of Shanghai Municipality (Grants Nos. 06dj14005 and 08DZ1150302) and National Basic Research Program of China (No. 2007CB613703) are acknowledged for their financial support. The authors are grateful to Robert Kubic (GM R&D Center, Warren, MI, USA) for technical assistance on EBSD, and Alan A. Luo (GM R&D Center, Warren, MI, USA) for discussion.

References

[1] S.R. Agnew, M.H. Yoo, C.N. Tome, Acta Mater. 49 (2001) 4277.
[2] L. Jin, W.Y. Wu, R.K. Mishra, A.A. Luo, A.K. Sachdev, S.S. Yao, TMS (The Minerals, Metals & Materials Society), 2009, p. 429.
[3] Y.N. Wang, J.C. Huang, Mater. Chem. Phys. 81 (2003) 11.
[4] Q.L. Jin, S. Shim, S. Lim, Scripta Mater. 55 (2006) 843.
[5] H. Li, E. Hsu, J. Szpunar, E. Verma, J. Carter, J. Mater. Eng. Perform. 16 (2007) 321.
[6] J.A. del Valle, F. Carreño, O.A. Ruano, Acta Mater. 54 (2006) 4247.
[7] R. Ohyama, et al., Magnesium Alloys 2003, Materials Science Forum, Trans Tech, Switzerland, 419–422, 2003, pp. 189–194 and pp. 237–242.
[8] J. Koike, et al., Mater. Trans. 44 (2003) 445.
[9] A.K. Mukherjee, M.G. Zelin, R.Z. Valiev, Mater. Sci. Eng. A 158 (1992) 165.
[10] C.S. Roberts, The deformation of magnesium, in: Magnesium and Its Alloys, Wiley, New York, 1960.
[11] B.C. Wonsiewicz, E.A. Backofen, Trans. TMS AIME 239 (1967) 1422.
[12] G.I. Taylor, J. Inst. Met. 62 (1938) 307.
[13] L. Jiang, J.J. Jonas, R.K. Mishra, A.A. Luo, A.K. Sachdev, S. Godet, Acta Mater. 55 (2007) 3899.
[14] L. Jin, D.L. Lin, D.L. Mao, X.Q. Zeng, B. Chen, W.J. Ding, Mater. Sci. Eng. A 423 (2006) 247.
[15] F.J. Humphreys, M. Hatherly, Recrystallization and Related Annealing Phenomena, Printed and bound in Great Britain by Galliard (printers) Ltd., 1995, p. 363.
[16] D. Kuhlmann-Wilsdorf, Scripta Mater. 36 (1997) 173.
[17] R.K. Mishra, A.K. Gupta, P.R. Rao, A.K. Sachdev, A.M. Kumar, A.A. Luo, Scripta Mater. 59 (2008) 562.
[18] S.R. Agnew, Ö. Duygulu, Int. J. Plasticity 21 (2005) 1161.